

HOW EXPONENTIALLY ILL-CONDITIONED ARE CONTIGUOUS SUBMATRICES OF THE FOURIER MATRIX?

ALEX H. BARNETT

Abstract. We show that the condition number of any cyclically contiguous $p \times q$ submatrix of the $N \times N$ discrete Fourier transform (DFT) matrix is at least

$$\exp\left(\frac{\pi}{2}\left[\min(p, q) - \frac{pq}{N}\right]\right),$$

up to algebraic prefactors. That is, fixing any shape parameters $(\alpha, \beta) := (p/N, q/N) \in (0, 1)^2$, the growth is $e^{\rho N}$ as $N \rightarrow \infty$ with rate $\rho = \frac{\pi}{2}[\min(\alpha, \beta) - \alpha\beta]$. Such Vandermonde system matrices arise in many applications, such as Fourier continuation, super-resolution, and diffraction imaging. Our proof uses the Kaiser–Bessel transform pair (of which we give a self-contained proof) and estimates on sums over distorted sinc functions, to construct a localized trial vector whose DFT is also localized. We warm up with an elementary proof of the above but with *half* the rate, via a periodized Gaussian trial vector. Using low-rank approximation of the kernel e^{ixt} , we also prove another lower bound $(4/e\pi\alpha)^q$, up to algebraic prefactors, which is stronger than the above for small α, β . When combined, the bounds are within a factor of two of the numerically-measured empirical asymptotic rate, uniformly over $(0, 1)^2$, and they become sharp in certain regions. However, the results are not asymptotic: they apply to essentially all N, p , and q , and with all constants explicit.

1. Introduction and main results. The size- N discrete Fourier transform (DFT) matrix F has elements

$$F_{jk} = e^{2\pi ijk/N}, \quad j, k \in \mathbb{Z}, \quad -N/2 \leq j, k < N/2, \quad (1.1)$$

where the row and column index sets should be taken as N -periodic; we center them on zero for convenience later.¹ Taking the DFT of a vector in \mathbb{C}^N , for instance via the fast Fourier transform (FFT) algorithm, is equivalent to multiplication by F . That F is full rank and its matrix condition number, $\text{cond}(F)$, is 1 follows from the unitarity of F/\sqrt{N} . However, it is well known that contiguous submatrices of F of size $p \times q$ are approximately low rank, with ϵ -rank of order pq/N [13, 31, 41]. On the other hand, their condition number must be finite, because any submatrix (or its adjoint) may be obtained by deleting columns of a Vandermonde, hence nonsingular, matrix $(z_j^k$ for the nodes $z_j = e^{2\pi ij/N}$). Yet, Vandermonde matrices are suspected to be exponentially ill-conditioned unless nodes are equispaced over the entire unit circle [33]. This leads one naturally to ask: how do the condition numbers of Fourier submatrices behave? Their growth has been established to be exponential [29, Thm. 3.1], and preliminary study exists for the case $p = q = N/2$ [33, Thm. 6.2 and Table 4]. Yet, what is the exponential *rate*, and how does it depend on p and q ? Figure 1.1 illustrates this growth, and hints at a *universal* rate depending only on the scaled submatrix shape. There appear to have been few rigorous answers to these quite simple and fundamental questions.

The conditioning of Fourier submatrices has consequences in applications because it controls the numerical stability, or noise amplification, of various function and image reconstruction problems:

1. In Fourier extension (or continuation) methods [8, 20, 27], with applications including the numerical solution of PDEs [2], Fourier series coefficients are solved by collocation on a grid covering a *fraction* of the periodic interval. In

¹Note that when N is even each set is $\{-N/2, \dots, N/2 - 1\}$, whereas when N is odd it is $\{-(N-1)/2, \dots, (N-1)/2\}$.

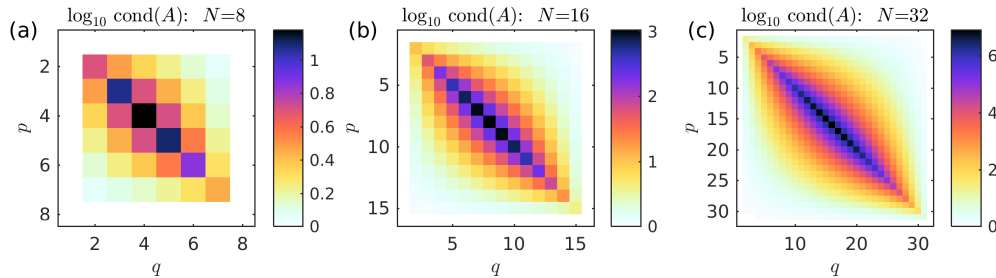


FIG. 1.1. Condition numbers of all possible submatrices A of the size- N Fourier matrix F , as a function of their size $p \times q$. Panels (a–c) compare this for three increasing N values, which are still rather small. Each vertical (p) axis is oriented downwards to match the usual sense for matrices. The color scale is logarithmic, illustrating exponential growth both in N , and as (p, q) tends to the diagonal. See Figure 4.1 for a study of the $N \rightarrow \infty$ exponential rates and comparison to lower bounds proven in this work. The diagonal symmetry $p \leftrightarrow q$ is exact for each N , but the inversion symmetry $(p, q) \leftrightarrow (N - p, N - q)$ is only true asymptotically as $N \rightarrow \infty$ (see Section 5.2).

the common case of a uniform grid, the system matrix is a contiguous submatrix of F with shape parameter $\alpha := p/N$ equal to the covered fraction, and $\beta := q/N$ equal to this fraction divided by the oversampling.² The apparent exponential ill-conditioning is well documented [8, 9] [1, Fig. 13]. However Adcock et al. [1] concluded, “there is no existing analysis [of submatrices of F] akin to that of Slepian’s for the prolate matrix...”. Zhu et al. [41] have since supplied one such missing piece; this paper supplies another.

2. Super-resolution imaging has importance in microscopy, astronomy, radar, and medicine (see [12, 11, 29, 26, 5] and references within). Even when source locations are known, and other fascinating issues such as sparsity and clustering are put aside, a linear system must be solved for the amplitudes, given known Fourier series coefficients (in the discrete model) up to some bandlimit p . A pathological arrangement for q such sources is a regular grid (“clump”) with spacing some factor (the so-called SRF [12, 11, 5]) times smaller than the Nyquist spacing. The system matrix becomes a $p \times q$ Fourier submatrix, with $\alpha = 1/\text{SRF}$, and the exponential blow-up of its conditioning is a fundamental obstacle in the presence of noise.
3. In coherent X-ray diffraction imaging, the data are squared magnitudes of the Fourier transform of an unknown image [28, 7]. This data often excludes a region around the \mathbf{k} -space origin, due to excessive intensity. However, since such data are also the Fourier transform of the image *autocorrelation*, such missing data may be recovered by solving a linear system involving a Fourier submatrix [3]. In the one-dimensional (1D) model, $q \ll N$ is then the number of missing data, and $\alpha = 1 - 2/m$ where $m > 2$ is an oversampling factor. The recovered data can help with the subsequent phase retrieval problem; this motivated the present study.

More widely, linear systems involving rectangular Vandermonde matrices arise in a variety of signal processing and parameter identification problems [6, 26]. The square of the singular values of Fourier submatrices are the eigenvalues controlling the maximum space- and frequency-concentration of *periodic discrete prolate spheroidal*

²Specifically, $\alpha = 1/T$ and $\beta = 1/\gamma T$ in the notation of [1, §5].

sequences (P-DPSS) [19, 21, 27, 41], the fully discrete ($\mathbb{C}^N \rightarrow \mathbb{C}^N$) analogues of prolate spheroidal wavefunctions [36, 32]. As Zhu et al. [41] state, “there exist comparatively few results concerning the P-DPSS eigenvalues.”

1.1. Results. Each of our three results is a lower bound on the condition number of contiguous Fourier submatrices, that, barring algebraic prefactors, is exponential in the submatrix size. Each bound has all constants explicit. To provide insight, we also present these as $N \rightarrow \infty$ asymptotic rates when the shape parameters (α, β) are held fixed (Table 1.1). Yet we emphasize that the main theorems are *not asymptotic results*—in particular, between them they cover all N and, using the $p \leftrightarrow q$ symmetry of the condition number, all p and q .

We include our first result, even though it will be essentially superceded by Theorem 2, because its prefactor is slightly stronger, and moreover its elementary proof (Section 2) is instructive.

THEOREM 1. *Let A be a cyclically contiguous $p \times q$ submatrix of the $N \times N$ discrete Fourier matrix F given by (1.1), with $2 < q \leq p < N - 2$. Then the condition number of the matrix A obeys*

$$\text{cond}(A) \geq \frac{\sqrt{\bar{p}}(1 - \bar{p}/N)^{1/4}}{6\bar{q}^{1/4}\sqrt{N}} e^{\frac{\pi}{4}(1 - \bar{p}/N)\bar{q}}. \quad (1.2)$$

where \bar{q} is the largest even integer smaller than q , and \bar{p} is the smallest integer of the same parity as N larger than p .

This applies to the square or “tall” case $q \leq p$; if instead $q > p$ (the submatrix is “fat”), one applies this theorem to its Hermitian adjoint A^* , since $\text{cond}(A^*) = \text{cond}(A)$. It is thus possible to rephrase the theorem (and the two below) in a symmetrized form that applies without such conditions on p and q . We will do this in terms of fixed fractional sizes or shape parameters $\alpha := p/N$ and $\beta := q/N$. Since $q - \bar{q}$ and $p - \bar{p}$ are at most 2, they may be absorbed into a prefactor. Thus,³

$$\text{cond}(A) = \Omega(N^{-1/4} e^{\rho(\alpha, \beta)N}), \quad N \rightarrow \infty$$

where the rate ρ , and the implied constant, depend on α and β . Explicitly, $\rho(\alpha, \beta) = \frac{\pi}{4}\beta(1 - \alpha)$ if $\beta \leq \alpha$. Combining this with the case $\beta > \alpha$ by swapping α and β , we get the rate $\rho = \frac{\pi}{4}[\min(\alpha, \beta) - \alpha\beta]$ applying for all $(\alpha, \beta) \in (0, 1)^2$. These two forms are summarized in the first row of Table 1.1.

Our next result is similar but has a *doubled* rate, and a more involved proof (Section 3). Here I_0 will denote the modified Bessel function of order zero [30, (10.25.2)].

THEOREM 2. *Let A be a cyclically contiguous $p \times q$ submatrix of the $N \times N$ Fourier matrix, with $1 \leq q \leq p < N$. Then*

$$\text{cond}(A) \geq \frac{I_0\left(\frac{\pi}{2}(1 - p/N)q\right) - 1}{2(\sqrt{N/p} + 6q)}. \quad (1.3)$$

Using the asymptotic $I_0(z) \sim e^z/\sqrt{2\pi z}$ given in [30, (10.3.4)], and keeping only dominant terms, we get, in terms of the shape parameters,

$$\text{cond}(A) = \Omega(N^{-3/2} e^{\rho(\alpha, \beta)N}), \quad N \rightarrow \infty$$

³Here we use the Ω symbol in the lower bound or Knuth sense that the right-hand side is \mathcal{O} of the left-hand side.

| theorem | rate ρ for $\beta \leq \alpha$ | rate ρ in general [†] | proof technique and section |
|---------|-------------------------------------|---|--|
| Thm. 1 | $\frac{\pi}{4}\beta(1-\alpha)$ | $\frac{\pi}{4}[\min(\alpha, \beta) - \alpha\beta]$ | periodized Gaussian trial (Sec. 2) |
| Thm. 2 | $\frac{\pi}{2}\beta(1-\alpha)$ | $\frac{\pi}{2}[\min(\alpha, \beta) - \alpha\beta]$ | periodized Kaiser–Bessel trial (Sec. 3) |
| Thm. 3 | $\beta \log \frac{4}{e\pi\alpha}$ | $\min(\alpha, \beta) \log \frac{4}{e\pi \max(\alpha, \beta)}$ | low-rank e^{ixt} kernel approx. (Sec. 4) |

TABLE 1.1

Summary of exponential growth rates $\rho = \rho(\alpha, \beta)$ of the lower bound $e^{\rho N}$ on the condition number of a $p \times q$ contiguous submatrix of the $N \times N$ Fourier matrix, as a function of fixed shape parameters $\alpha := p/N$ and $\beta := q/N$, asymptotically as $N \rightarrow \infty$. We drop algebraic prefactors, and drop $\mathcal{O}(1)$ changes in p, q , since we assume $p, q \gg 1$. Each row summarizes a different theorem proven in this paper. The second column presents the simpler “non-fat” $q \leq p$ submatrix case, and the third column the general case. The [†] is a reminder that Theorem 3 only applies for $\alpha, \beta < 4/e\pi \approx 0.468$.

with an explicit rate ρ precisely double that from the first theorem, for each α and β . This is summarized in the abstract, and in the second row of Table 1.1.

Our final main result (proved in Section 4) improves upon the above in the case of small α and β , i.e., in the “corner” of (α, β) space.

THEOREM 3. *Let A be a cyclically contiguous $p \times q$ submatrix of the $N \times N$ Fourier matrix, with $1 < q \leq p < 4N/e\pi + 1$. Then*

$$\text{cond}(A) \geq \frac{1 - (e\pi(p-1)/4N)}{2\sqrt{q}} \left(\frac{4N}{e\pi(p-1)} \right)^{q-1}. \quad (1.4)$$

When $p, q \gg 1$ it again makes sense to approximate $p-1$ by p , and $q-1$ by q , and rephrase this in terms of the shape parameters, giving

$$\text{cond}(A) = \Omega(N^{-1/2} e^{\rho(\alpha, \beta)N}), \quad \alpha, \beta < 4/e\pi \approx 0.468, \quad N \rightarrow \infty$$

with $\rho = \beta \log(4/e\pi\alpha)$ when $\beta \leq \alpha$. Its symmetrized form is listed on the last row of Table 1.1.

When is Theorem 3 stronger than Theorem 2? Equating their rates $\beta \log(4/e\pi\alpha) = \rho = \frac{\pi}{2}\beta(1-\alpha)$ gives a transcendental equation in α with solution $\alpha_* \approx 0.117$. Including the symmetrized result, Theorem 3 is then stronger for all $(\alpha, \beta) \in (0, \alpha_*)^2$, i.e., in the corner region occupying about 1.4% of shape space. (In Section 5.2 it is shown how this result also applies asymptotically to $(1-\alpha, 1-\beta)$, hence also in the diagonally-opposite corner.)

In summary, Table 1.1 compares the exponential rates ρ in these three theorems, dropping the algebraic prefactors. Remark 4 below shows that Theorem 2 tends to have a sharp rate at $(1, 0)$ and $(0, 1)$. Figure 4.1 compares the rates from Theorem 2 (see panels (b,e)) and Theorem 3 (panel (e)) against the *empirical* numerical growth rate of $\text{cond}(A)$, denoted by $\tilde{\rho}(\alpha, \beta)$. In short (see Section 5.1), the lower bound from the stronger of these two theorems appears to be within a factor of 2 of the empirical rate uniformly over shape space $(0, 1)^2$.

1.2. Relation to prior work. Here we compare our findings to the few existing lower bounds on the condition number. At the end of this section we discuss an asymptotic connection to eigenvalues of the prolate matrix. We also note that there have been a couple of small-scale numerical studies [1, Fig. 13] [33, Table 4] [26, Fig. 4(a)].

The foundational work of Edelman–McCorquodale–Toledo [13, Thm. 3] showed that square Fourier submatrices A with $\alpha = \beta = 1/n$, $n = 2, 3, \dots$, have an ϵ -rank of

$\alpha^2 N$, asymptotically as $\alpha N \rightarrow \infty$. However, their analysis did not access $\text{cond}(A)$. Recently Zhu et al. [41, Cor. 1] gave a more refined ϵ dependence of the asymptotic distribution of singular values of such an A . They show that $\sigma_j(A) \leq \epsilon$ for $j \geq j_\epsilon$, with a formula for j_ϵ that is at least⁴ $\alpha^2 N + (\frac{4}{\pi^2} \log 8\alpha N + 6) \log(16/\epsilon^2)$. To convert this to a lower bound on condition number one equates j_ϵ to αN , the submatrix size, then solves for ϵ . Simplifying somewhat, the resulting lower bound cannot be stronger than

$$\text{cond}(A) \sim \epsilon^{-1} \gtrsim \exp\left[\frac{\alpha(1-\alpha)}{(8/\pi^2) \log 8\alpha N + 12} N\right],$$

which is super-algebraic, but falls short of $e^{\rho N}$ for any positive ρ .

To our knowledge, the chief prior exponential lower bounds on $\text{cond}(A)$ are the following three.

1) Pan [33, Thm. 6.2] proves that for $p = q = N/2$, $\text{cond}(A) \geq \sqrt{N} 2^{N/4-1}$, i.e. $\rho = (\log 2)/4 \approx 0.173$. We see that both Theorems 1 and 2 are stronger than this, the latter giving $\rho = \pi/8 \approx 0.393$ at $\alpha = \beta = 1/2$.

2) Moitra [29, Thm. 3.1] gives the only proof of which we are aware that the condition number of a submatrix of *general* shape grows at least exponentially, although no rate is given. His method is similar to that of our Theorem 2—although we found it independently—but with trial vector \mathbf{v} chosen as a high power of the Fejér kernel. By tracking the rate in his proof⁵ we get, in our notation,

$$\rho_{\text{Moitra}} = (\log \sqrt{2})\beta(1-\alpha), \quad \beta \leq \alpha.$$

This has a similar form as our first two theorems (see Table 1.1), but Theorem 2 improves upon it by a factor of about 4.5, for all (α, β) .

3) In the super-resolution literature, lower bounds on the condition number have been proven in the case of fixed q , and $\alpha \ll 1$. They take the general form $\text{cond}(A) \geq (c\alpha)^{-q+1} \propto e^{\beta N \log(1/c\alpha)}$, similar to the last row of our Table 1.1. The strongest such result that we know of is that of Li-Liao [26] (see also [24, Ex. 5.1]). In our notation, [26, Prop. 3] states

$$\sigma_{\min}(A) \leq \binom{2q-2}{q-1}^{-1/2} 2\sqrt{p}(2\pi\alpha)^{q-1} \leq \sqrt{8pq}(\pi\alpha)^{q-1}, \quad (1.5)$$

where in the second form we bounded the central binomial coefficient. Thus their constant is $c = \pi$. Their proof exploits the q th-order finite difference trial vector $v_j = (-1)^j (q-1)! / (q-j)!(j-1)!$, $j = 1, \dots, q$, whose first q moments vanish, following Donoho [12, §7.4]. The result (1.5) has restrictive conditions: $\alpha \leq 1/(C(q)\sqrt{p})$, where one may check that $C(q) \sim 4^q$. Thus (1.5) does not apply for fixed q and α as $N \rightarrow \infty$. In contrast, our Theorem 3 applies to all submatrix sizes up to $0.468N$, and furthermore its rate constant c is $4/e \approx 1.47$ times stronger.

REMARK 4 (The prolate matrix and sharpness). *There is a limit in which the singular values of A are already well understood [13, 1, 41, 5]. When $N \rightarrow \infty$ with α and q held constant (so that the height of A is much larger than its width), a Riemann sum shows that A^*A tends to a multiple of Slepian's prolate matrix [35, 40]. The latter*

⁴Here for simplicity we ignore their nonnegative second term in $R(L, M, \epsilon)$.

⁵Note that his short proof is unclear about whether the width ℓ and power r may be non-integer-valued, which would be needed to make claims for almost all p and q , as we do.

is $P(q, \alpha/2)$ in standard notation, with elements $(P(q, \alpha/2))_{jk} = \alpha \operatorname{sinc}(\pi\alpha(j-k))$, $j, k = 1, \dots, q$, recalling that $\operatorname{sinc} x := (\sin x)/x$ for $x \neq 0$ and 1 otherwise. Thus, in this limit, the singular values of A are the square-roots of the eigenvalues of $P(q, \alpha/2)$. Slepian proved the $q \rightarrow \infty$ asymptotic for the smallest such eigenvalue [35, Eqs. (13), (58)],

$$\lambda_0(P(q, \alpha/2)) = 1 - \lambda_{q-1}(P(q, (1-\alpha)/2)) \sim 2^{9/4} \sqrt{\pi q} \frac{(1 - \cos \pi\alpha)^{1/4}}{(1 + \cos \pi\alpha)^{1/2}} \theta^{-q}$$

where $\theta = \cot^2(\pi\alpha/4) \in (1, \infty)$ [1, §3.2]. Recalling that $q = \beta N$, the term θ^{-q} predicts an exponential growth rate for $\operatorname{cond}(A)$ of

$$\rho_{\text{prolate}} := \beta \log \cot \frac{\pi\alpha}{4}, \quad \beta \ll \alpha, \quad (1.6)$$

which should be compared with our results in the second column of Table 1.1.

In particular, the first term in the Taylor expansion of (1.6) about $\alpha = 1$ is precisely our $\frac{\pi}{2}\beta(1-\alpha)$, proving that as $\alpha \rightarrow 1^-$ and $\beta \ll 1$, the rate in Theorem 2 is sharp. Instead taking $\alpha \rightarrow 0^+$ gives $\beta \log(4/\pi\alpha)$, indicating that the rate of Theorem 3 fails to be sharp by an amount β . We have also checked that for $\beta \ll \alpha$ the empirical rates shown in Figure 4.1(a) match (1.6) very well: the agreement is within 0.05 uniformly over $0 < \alpha < 1$, $0 < \beta < \alpha/3$.

We emphasize that, in contrast to the above prolate asymptotics which fix q and α with $N \rightarrow \infty$, our Theorems 1–3 are *not* asymptotic: they apply to arbitrary N and essentially arbitrary p and q .

1.3. Overview of proof methods. We now outline the tools used to prove the three main theorems. The definition of matrix condition number is

$$\operatorname{cond}(A) := \frac{\sigma_1(A)}{\sigma_{\min}(A)}, \quad (1.7)$$

where $\sigma_1 \geq \sigma_2 \geq \dots \geq \sigma_{\min(p,q)} =: \sigma_{\min}$ are the singular values of A . All three proofs place exponentially small upper bounds on $\sigma_{\min}(A)$, then combine this with the following simple bound.

PROPOSITION 5. *The largest singular value of any $p \times q$ submatrix of the Fourier matrix (1.1) obeys*

$$\sigma_1(A) \geq \sqrt{p}. \quad (1.8)$$

Proof. The operator norm of A is bounded by the Frobenius norm [17, (2.3.7)] giving, $\sqrt{pq} = \|A\|_F \leq \sqrt{q}\|A\|$. The result follows since $\sigma_1(A) = \|A\|$. \square

Theorems 1 and 2 will use the variational bound on σ_{\min} . Namely, if $q \leq p$, then

$$\sigma_{\min}(A) = \sigma_q \leq \frac{\|A\mathbf{v}\|_2}{\|\mathbf{v}\|_2}, \quad \text{for any } \mathbf{v} \in \mathbb{C}^q, \mathbf{v} \neq \mathbf{0}. \quad (1.9)$$

If instead $q > p$ (a “fat” submatrix), (1.9) no longer holds, explaining the hypothesis $q \leq p$ in Theorems 1 and 2.

Our trick to construct a trial vector \mathbf{v} for which $A\mathbf{v}$ is nearly (or exactly) known is by *embedding* this matrix-vector product in the larger one, $F\mathbf{f}$, for some $\mathbf{f} \in \mathbb{C}^N$. Firstly we note that cyclic horizontal or vertical translations of the submatrix location

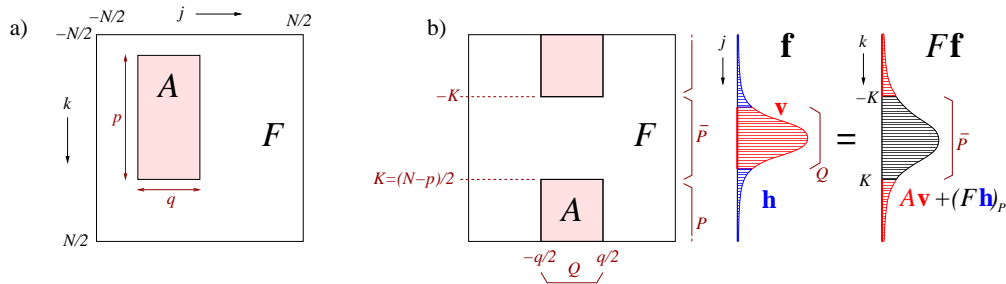


FIG. 1.2. The main proof idea for Theorems 1 and 2. a) shows the submatrix A (pink) within the $N \times N$ Fourier matrix F . b) shows the cyclically shifted A (pink) again within F , and the formation of the DFT matrix-vector product $F\mathbf{f}$. The vector \mathbf{f} is exponentially small outside of the central index set Q , and has a known DFT which is exponentially small in the high frequency index set P . The length- q vector (shown in red) is $\mathbf{v} = \mathbf{f}|_Q$, i.e., restricted to the “input” indices. $F\mathbf{f}$ in the “output” index set P equals $A\mathbf{v}$ plus a correction $(F\mathbf{h})|_P$, where \mathbf{h} (shown blue) is the part of \mathbf{f} outside of Q . For Theorem 1, \mathbf{f} samples a periodized Gaussian (as sketched); for Theorem 2 it samples a periodized “deplined” Kaiser–Bessel function (see Figure 3.1; in this case $\mathbf{h} = \mathbf{0}$).

within F do not affect its singular values. This can be seen by noting that a cyclic right-translation by m of a submatrix A is equivalent to left-multiplication of A by the diagonal unitary matrix with diagonal entries $\{e^{2\pi ijm}\}_{j \in J}$, where J is the set of row indices of A (this has been pointed out, e.g., in [41, Sec. III.C]). Thus we translate the index sets of A to be the p highest magnitude output frequencies (see P defined by (2.9)), and the q lowest-magnitude inputs $Q := \{j \in \mathbb{Z} : -q/2 \leq j < q/2\}$; see Figure 1.2. The trial vector \mathbf{v} will then be $\mathbf{f}|_Q$, the restriction of \mathbf{f} to the central index set Q . The desired $A\mathbf{v}$ is then $(F\mathbf{f})|_P$, plus a correction of size at most the norm of \mathbf{f} outside Q , which is arranged to be small or zero.

Thus we seek an \mathbf{f} that is exponentially small outside of Q , whose DFT, $F\mathbf{f}$, is known and exponentially small in P . We build this from a known Fourier transform pair $f(t)$ and $\hat{f}(\omega)$ on \mathbb{R} , by applying the phased variant of the Poisson summation formula [38, Thm. 3.1]

$$\sum_{j \in \mathbb{Z}} e^{2\pi i j \omega} f(j) = \sum_{m \in \mathbb{Z}} \hat{f}(\omega + m). \quad (1.10)$$

Setting $\omega = k/N$ makes the left-hand side equal to the k th entry of $F\mathbf{f}$, for a vector \mathbf{f} whose j th entry is $f_j = \sum_{n \in \mathbb{Z}} f(j + nN)$, a sample of the N -periodization of the original function f .

In Theorem 1 we choose the Gaussian Fourier pair, which is of course well localized both in position and frequency space. It also has monotonic tails, allowing sums to be bounded by simple integrals. However, the problem of *optimal* (in the $L^2(\mathbb{R})$ sense) simultaneous position- and frequency-localization was solved by Slepian and co-workers in the form of the prolate spheroidal wavefunctions (PSWFs) of order zero, in particular the first such function ψ_0 [36, 25, 32]. Thus one might hope that by choosing f as a scaled truncated ψ_0 , making \hat{f} a scaled (but not truncated) ψ_0 , one could beat the Gaussian rate. Yet, we were unable to find estimates on the tails of ψ_0 that enable bounding the right-hand side sum in (1.10). Instead, Theorem 2 relies on the so-called Kaiser–Bessel (KB) Fourier transform pair [22, 15] defined by (3.2), which has the same optimal exponential rate of localization as the PSWF (see, e.g., [4, Sec. 5]). The non-compactly-supported member of this pair involves only sinc

and other elementary functions, allowing a bound on its tail sum. Since the tail is *oscillatory* rather than monotonic (see Figure 3.1), the bound is involved, although elementary. Here we draw on the thesis of Fourmont [14]; he was concerned with error of the nonuniform FFT [15, 23, 4] where the criteria for a good spreading kernel are similar to those for f . We suspect that this work is the first to exploit the KB pair as an *analysis* (as opposed to numerical) tool.

In contrast, to prove Theorem 3, σ_{\min} is bounded from above via the SVD rank approximation theorem⁶ [17, Thm. 2.5.3]. Namely, σ_q is bounded from above by the error of any rank- $(q - 1)$ approximation of A , in the operator norm. A rapidly-convergent approximation comes by sampling a carefully chosen continuous kernel expansion of the form

$$e^{ixt} = \sum_{n=1}^{\infty} f_n(x)g_n(t)$$

on regular grids in x and t , so that its samples give the elements of A . This sampling idea has been used by O’Neil–Rokhlin to bound the numerical rank of A [31, Cor. 3.4].

The structure of the rest of this paper is as follows. The next three sections correspond to the three main theorems: Section 2 proves the elementary Gaussian rate, Section 3 proves the doubled rate based on the Kaiser–Bessel pair, then Section 4 proves the further improved rate in the corner region of the (α, β) plane. Finally, Section 5 has a detailed numerical comparison to the empirical growth rate, discusses symmetries (both exact and near) in the (α, β) plane, and draws some conclusions. A short Appendix proves the Kaiser–Bessel transform pair.

2. Proof of elementary Gaussian rate (Theorem 1). We start with a simple identity that the DFT of a periodized discrete Gaussian is another periodized discrete Gaussian.

PROPOSITION 6. *Let $N \in \mathbb{N}$, $\sigma > 0$, and define the N -periodic vector $\mathbf{f} \in \mathbb{C}^N$ by its entries*

$$f_j = \sum_{n \in \mathbb{Z}} e^{-\frac{1}{2}(j+nN)^2/\sigma^2}, \quad -N/2 \leq j < N/2. \quad (2.1)$$

Then the k th component of the DFT of \mathbf{f} is

$$(F\mathbf{f})_k = \sqrt{2\pi}\sigma \sum_{m \in \mathbb{Z}} e^{-2(\pi\sigma/N)^2(k+mN)^2}, \quad -N/2 \leq k < N/2. \quad (2.2)$$

Proof. With the (“number theorist”) Fourier transform convention

$$\hat{f}(\omega) := \int_{\mathbb{R}} f(t)e^{2\pi i\omega t} dt, \quad \omega \in \mathbb{R} \quad (2.3)$$

we have the usual continuous Fourier transform pair

$$f(t) = e^{-\frac{1}{2}(t/\sigma)^2} \quad \longleftrightarrow \quad \hat{f}(\omega) = \sqrt{2\pi}\sigma e^{-2(\pi\sigma\omega)^2}. \quad (2.4)$$

Inserting this f into the Poisson summation formula (1.10) and setting $\omega = k/N$ gives the discrete sums

$$\sum_{j \in \mathbb{Z}} e^{2\pi ijk/N} e^{-\frac{1}{2}(j/\sigma)^2} = \sqrt{2\pi}\sigma \sum_{m \in \mathbb{Z}} e^{-2(\pi\sigma)^2(k/N+m)^2}, \quad \forall k \in \mathbb{N}.$$

⁶This is often referred to as the Eckhart–Young theorem, although it is due to Schmidt.

By grouping terms with the same index modulo N , and using (1.1) and (2.1), the left-hand side can be seen to be $(F\mathbf{f})_k$. \square

PROPOSITION 7. (2.1) and (2.2) may be bounded uniformly over their centered index ranges by (non-periodic) Gaussians, namely

$$f_j \leq \left(2 + \sqrt{2\pi} \frac{\sigma}{N}\right) e^{-\frac{1}{2}(j/\sigma)^2}, \quad -N/2 \leq j < N/2. \quad (2.5)$$

$$(F\mathbf{f})_k \leq (\sqrt{8\pi}\sigma + 1)e^{-2(\pi\sigma k/N)^2}, \quad -N/2 \leq k < N/2. \quad (2.6)$$

Proof. Assume $j \geq 0$, then we may drop the cross-term in the square, then exploit monotonicity to bound a Gaussian sum by its integral, to get

$$\begin{aligned} \sum_{n \geq 0} e^{-\frac{1}{2}(j+nN)^2/\sigma^2} &\leq e^{-\frac{1}{2}(j/\sigma)^2} \sum_{n \geq 0} e^{-\frac{1}{2}(nN/\sigma)^2} \\ &\leq e^{-\frac{1}{2}(j/\sigma)^2} \left(1 + \int_0^\infty e^{-\frac{1}{2}(tN/\sigma)^2} dt\right) \leq e^{-\frac{1}{2}(j/\sigma)^2} \left(1 + \sqrt{\frac{\pi}{2}} \frac{\sigma}{N}\right). \end{aligned}$$

The negative terms are handled by shifting the sum

$$\sum_{n < 0} e^{-\frac{1}{2}(j+nN)^2/\sigma^2} = \sum_{n \geq 0} e^{-\frac{1}{2}(N-j+nN)^2/\sigma^2},$$

which, since $j \leq N/2$, is termwise no larger than the non-negative sum, giving an overall factor of two, hence (2.5). The $j < 0$ case is handled by noting $f_{-j} = f_j$. (2.6) follows by an identical method. \square

LEMMA 8. Let A be a cyclically contiguous $p \times q$ submatrix of the $N \times N$ discrete Fourier matrix F , with $p \geq q$ (i.e., the submatrix is either square or “tall”), $q > 2$, and $p < N - 2$. Then, in terms of \bar{p} and \bar{q} in Theorem 1, the smallest singular value of A obeys

$$\sigma_{\min}(A) \leq 6 \left(\frac{\bar{q}}{1 - \bar{p}/N}\right)^{1/4} \sqrt{N} \cdot e^{-\frac{\pi}{4}\bar{q}(1 - \bar{p}/N)}. \quad (2.7)$$

Proof. As discussed in Section 1.3, we translate A to be centered vertically about the highest frequency and horizontally about the lowest; see Figure 1.2(b). We then apply (1.9), with \mathbf{v} chosen as follows. We select the central q elements of \mathbf{f} , given by (2.1), with width parameter $\sigma > 0$ to be specified later, i.e.,

$$\mathbf{v} := \{f_j\}_{-q/2 \leq j < q/2}. \quad (2.8)$$

Let $\mathbf{g} \in \mathbb{C}^N$ be \mathbf{v} embedded in the vector of length N , i.e. with elements $g_j = f_j$ for $-q/2 \leq j < q/2$, zero otherwise. The remainder we denote by $\mathbf{h} \in \mathbb{C}^N$, that is, $h_j = 0$ for all $-q/2 \leq j < q/2$, and $h_j = f_j$ otherwise. In summary, $\mathbf{f} = \mathbf{g} + \mathbf{h}$, with \mathbf{g} supported only in the central region Q while \mathbf{h} is supported only in its complement; see Figure 1.2(b). Then, letting P be the (output) index set

$$P := \{-N/2 \leq k < -(N-p)/2\} \cup \{(N-p)/2 \leq k < N/2\}, \quad (2.9)$$

and using the inequality $(a - b)^2 < 2(a^2 + b^2)$, we bound

$$\begin{aligned} \|A\mathbf{v}\|_2^2 &= \sum_{k \in P} |(F\mathbf{g})_k|^2 = \sum_{k \in P} |(F\mathbf{f})_k - (F\mathbf{h})_k|^2 \\ &\leq 2 \sum_{k \in P} |(F\mathbf{f})_k|^2 + 2\|F\mathbf{h}\|_2^2 \leq 2 \sum_{k \in P} |(F\mathbf{f})_k|^2 + 2\|F\|^2\|\mathbf{h}\|_2^2. \end{aligned} \quad (2.10)$$

To bound the first sum in (2.10) we set $K := (N - \bar{p})/2$ as a lower bound on the half-width of \bar{P} , the complement of P in the full set $\{-N/2 \leq k < N/2\}$. Using this and (2.6),

$$\begin{aligned} \sum_{k \in P} |(F\mathbf{f})_k|^2 &\leq \sum_{|k| > K, -N/2 \leq k < N/2} |(F\mathbf{f})_k|^2 \leq 2(\sqrt{8\pi\sigma} + 1)^2 \sum_{k=K+1}^{\infty} e^{-(2\pi\sigma k/N)^2} \\ &\leq 2(\sqrt{8\pi\sigma} + 1)^2 \sum_{\ell > 0} e^{-\left(\frac{2\pi\sigma}{N}\right)^2 (K^2 + \ell^2 + 2K\ell)} \\ &\leq 2(\sqrt{8\pi\sigma} + 1)^2 e^{-\left(\frac{2\pi\sigma K}{N}\right)^2} \sum_{\ell > 0} e^{-\left(\frac{2\pi\sigma \ell}{N}\right)^2} \\ &\leq 2(\sqrt{8\pi\sigma} + 1)^2 e^{-\left(\frac{2\pi\sigma K}{N}\right)^2} \int_0^{\infty} e^{-\left(\frac{2\pi\sigma x}{N}\right)^2} dx = 4\sqrt{\pi}\sigma N \left(1 + \frac{1}{\sqrt{8\pi\sigma}}\right)^2 e^{-\left(\frac{2\pi\sigma K}{N}\right)^2}. \end{aligned}$$

To bound the second term in (2.10), we use (2.5) and apply an identical method to get

$$\begin{aligned} \|\mathbf{h}\|_2^2 &= \sum_{j \notin Q} f_j^2 \leq \sum_{|j| > \bar{q}/2, -N/2 \leq j < N/2} f_j^2 \leq 2 \left(2 + \sqrt{2\pi} \frac{\sigma}{N}\right)^2 \sum_{j=\bar{q}/2+1}^{\infty} e^{-(j/\sigma)^2} \\ &\leq 4\sqrt{\pi}\sigma \left(1 + \sqrt{\frac{\pi}{2}} \frac{\sigma}{N}\right)^2 e^{-(\bar{q}/2\sigma)^2}. \end{aligned}$$

Substituting the last two results and $\|F\|^2 = N$ into (2.10) and gathering common terms gives

$$\|A\mathbf{v}\|_2^2 \leq 8\sqrt{\pi}N\sigma \left[\left(1 + \frac{1}{\sqrt{8\pi\sigma}}\right)^2 e^{-(2\pi\sigma K/N)^2} + \left(1 + \sqrt{\frac{\pi}{2}} \frac{\sigma}{N}\right)^2 e^{-\bar{q}^2/4\sigma^2} \right] \quad (2.11)$$

Choosing the width σ to balance the two exponential rates gives

$$\sigma^2 = \frac{\bar{q}}{2\pi(1 - \bar{p}/N)}. \quad (2.12)$$

We can now bound the prefactor $(1 + 1/\sqrt{8\pi\sigma})^2 \leq (1 + \sqrt{1 - \bar{p}/N}/2\sqrt{\bar{q}})^2 \leq 3$ using $\bar{q} \geq 1$ implied by the hypothesis $q > 2$. Also, by the arithmetic-geometric inequality, $(1 + \sqrt{\pi}\sigma/\sqrt{2}N)^2 \leq 2 + \pi\sigma^2/N^2 \leq 3$ since $N - \bar{p} \geq 1$ from the hypothesis $p < N - 2$. Substituting these and (2.12) into (2.11) gives

$$\|A\mathbf{v}\|_2^2 \leq 24\sqrt{2} \sqrt{\frac{\bar{q}}{1 - \bar{p}/N}} N e^{-\frac{\bar{q}}{2}(1 - \bar{p}/N)}. \quad (2.13)$$

Finally, the crude lower bound $\|\mathbf{v}\|_2^2 \geq 1$ results by keeping only the term $j = n = 0$ in the definition (2.1) of f_j . Combining this with the square-root of (2.13), and simplifying $\sqrt{24\sqrt{2}} < 6$, gives (2.7). \square

REMARK 9. *A similar proof idea—an explicit trial function (in their case a truncated Gaussian) that is near a function whose Fourier transform nearly has compact support—was used by Landau and Pollak in [25, Lem. 4] to show that the prolate eigenvalue μ_0 is exponentially close to 1.*

With σ_{\min} upper bounded by Lemma 8, and $\sigma_1 \geq \sqrt{p}$ by Proposition 5, Theorem 1 follows from inserting these two bounds into the definition of $\text{cond}(A)$, namely (1.7).

3. Proof of Kaiser–Bessel doubled rate (Theorem 2). Theorem 2 is an immediate consequence of the lower bound on $\sigma_1(A)$ (Proposition 5), and the following upper bound on $\sigma_{\min}(A)$.

THEOREM 10. *Let A be a cyclically contiguous $p \times q$ submatrix of the $N \times N$ discrete Fourier matrix F , with $1 \leq q \leq p < N$ (i.e., either square or “tall”). Then, expressed in terms of $\alpha := p/N \in (0, 1)$,*

$$\sigma_{\min}(A) \leq \frac{2\sqrt{N}(1 + 6\sqrt{\alpha}q)}{I_0\left(\frac{\pi}{2}(1 - \alpha)q\right) - 1}, \quad (3.1)$$

where I_0 is the modified Bessel function of the first kind of order zero.

Before proving this, we introduce the main tool. The Kaiser–Bessel analytic Fourier transform pair is, given a parameter $\sigma > 0$,

$$\phi(t) = \begin{cases} I_0(\sigma\sqrt{1-t^2}), & |t| \leq 1 \\ 0, & \text{otherwise,} \end{cases} \quad \longleftrightarrow \quad \hat{\phi}(\omega) = 2 \text{sinc} \sqrt{(2\pi\omega)^2 - \sigma^2}, \quad (3.2)$$

with the Fourier convention (2.3). Apparently due to B. F. Logan [16], it is stated without proof in [22, p. 232–233], and since has become popular for windowing and gridding in signal processing (see [15, 23, 4] and references within). Since it is not listed in standard tables, and we know of no published proof, we include one in the Appendix. The parameter σ may be interpreted as a “cut-off” frequency: for $2\pi|\omega| < \sigma$ the sinc (and hence sin) has imaginary argument so is exponentially large (around e^σ), whereas for all $2\pi|\omega| \geq \sigma$ it is bounded by 2.

Our precise choice of Fourier pair will be informed by the need to bound an infinite algebraic sum (1.10) over its frequency argument. Since ϕ in (3.2) is discontinuous at ± 1 (see Figure 3.1(a)), the tails of $\hat{\phi}$ have sinc-type oscillations whose amplitude decays only as $|\omega|^{-1}$ (see Figure 3.1(d)); thus such algebraic sums are not absolutely convergent, making the analysis tricky.

REMARK 11. *A very similar type of sum over the tails of the function $\hat{\phi}$ in (3.2) has already been bounded in a detailed analysis by Fourmont [14, 15]. However, he relies on the fact that his sum is over the tail of an algebraic series with zero offset, allowing him to build on the uniformly bounded Fourier series $\sum_{k>0} (\sin kx)/k = (\pi - x)/2$ for $0 < x < 2\pi$, zero for $x = 2\pi$. When series with arbitrary offset are instead allowed, as we will require, logarithmic divergence is possible, as shown by $\sum_{k>0} \sin(2\pi k + \pi/2)/k = \infty$.*

For this reason, in order to simplify the analysis we subtract a top-hat function of height 1 and width 2 from ϕ in (3.2) to give the “deplinthed” Kaiser–Bessel function, which, in contrast to ϕ , is continuous on \mathbb{R} . Since this subtraction causes a change in $\hat{\phi}$ of at most 2, it preserves its excellent Fourier localization. Now rescaling t so that

the support falls within a q -sized interval, the deplinthed KB pair becomes

$$f(t) = \begin{cases} I_0\left(\sigma\sqrt{1 - \left(\frac{2t}{q}\right)^2}\right) - 1, & |t| \leq q/2 \\ 0, & \text{otherwise,} \end{cases} \quad \hat{f}(\omega) = q \left[\text{sinc}\sqrt{(\pi q\omega)^2 - \sigma^2} - \text{sinc}\pi q\omega \right] \quad (3.3)$$

which will play the role of (2.4) in the following proof of Theorem 10. This pair is shown by Figure 3.1(a,b,e).

Proof. We apply Poisson summation (1.10) to the pair (3.3), and set $\omega = k/N$, to give an explicit formula for the action of the DFT on \mathbf{f} , the vector with entries $f_j = f(j)$, $-N/2 \leq j < N/2$, being the discrete samples of (3.3). This action is

$$(F\mathbf{f})_k = q \sum_{m \in \mathbb{Z}} \left[\text{sinc}\sqrt{(\pi q)^2(k/N + m)^2 - \sigma^2} - \text{sinc}\pi q(k/N + m) \right], \quad -N/2 \leq k < N/2. \quad (3.4)$$

As in the proof of Lemma 1, the submatrix A is now arranged to sit within F so that its input (column) index set is $-q/2 \leq j < q/2$, and the output (row) index set P is as in (2.9).

However, in contrast to the Gaussian case, σ may now be chosen up front, as follows. We need to ensure that for each index $k \in P$, all of the arguments in the terms in (3.4) fall at or beyond cutoff (see Figure 3.1(b)), so that their contribution is exponentially small relative to $\|\mathbf{f}\|$. It is sufficient to check this for the term $m = 0$, because $|k| \leq N/2$. This gives the criterion $\pi q|k|/N \geq \sigma$ for all $k \in P$. For all $k \in P$ we have $|k| \geq (N - p)/2 = (1 - \alpha)N/2$, so the choice

$$\sigma = \frac{\pi}{2}(1 - \alpha)q \quad (3.5)$$

optimally satisfies the criterion, and we fix this from now on.

In order to bound (3.4) we will break up the sum into two one-sided sums, each of which has the form

$$S_\sigma(a, b) := \sum_{m \geq 0} \text{sinc}\sqrt{(am + b)^2 - \sigma^2} - \text{sinc}(am + b), \quad (3.6)$$

where $a = \pi q$ is the spacing and b the offset for the arithmetic progression of frequencies $am + b$. Using the even symmetry of the sinc function, we now split the sum (3.4) into three parts, $m < 0$, $m > 0$, and $m = 0$, to get, in terms of (3.6), the three terms

$$(F\mathbf{f})_k = qS_\sigma\left(\pi q, \pi q\left(1 - \frac{k}{N}\right)\right) + qS_\sigma\left(\pi q, \pi q\left(1 + \frac{k}{N}\right)\right) + q \left[\text{sinc}\sqrt{(\pi qk/N)^2 - \sigma^2} - \text{sinc}(\pi qk/N) \right].$$

Here in both instances of the one-sided sum $S_\sigma(\pi q, b)$, the offset b obeys $b > \sigma$, because $|k| \leq N/2$ and $\sigma < \pi q/2$. Thus each sum satisfies the conditions of Lemma 13, stated and proved in the next subsection, which bounds it by

$$|S_\sigma(\pi q, b)| \leq \frac{5}{2\pi q\sqrt{\alpha}} + 5 < \frac{1}{q\sqrt{\alpha}} + 5, \quad (3.7)$$

uniformly over $k \in P$. From the above formula for $(F\mathbf{f})_k$, applying the triangle inequality, the fact that $|\text{sinc}y| \leq 1$ for $y \in \mathbb{R}$, then the bound (3.7), gives, for all

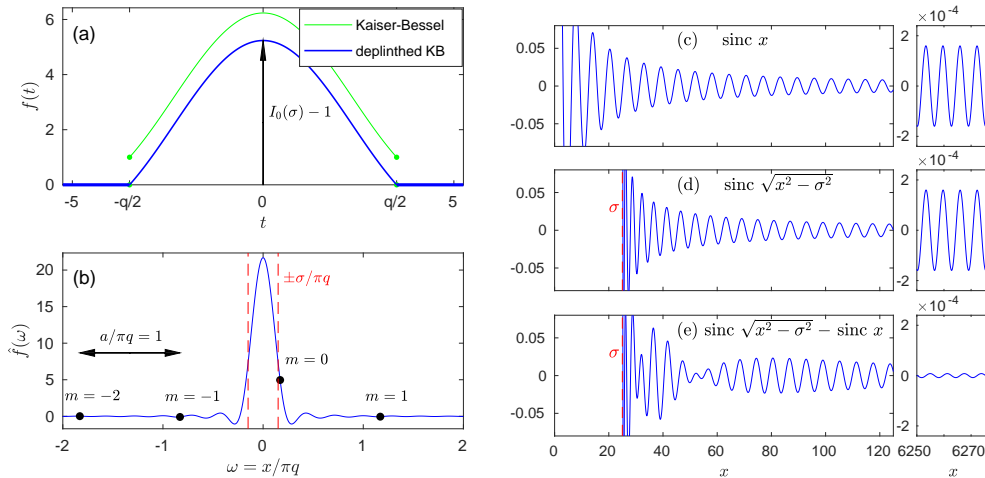


FIG. 3.1. Functions key to proving Theorem 2: deplined Kaiser–Bessel Fourier transform pair (left panels), and various sinc functions (right and far-right panels). (a) shows $f(t)$ from (3.3) (blue), and the KB function ($\phi(t)$ in (3.2) except scaled to have support $[-q/2, q/2]$, green). Here $q = 7$ (chosen small for easy visualization), and $\alpha = 0.7$. (b) shows $\hat{f}(\omega)$ from (3.3) (blue), the cutoff (dotted red), and the arithmetic progression $\omega = k/N + m$ (black dots) as in (3.4), for k just above $(1 - \alpha)N/2$. (c, d, e) compares the sinc, “warped” sinc, and their difference. (x will take the values $x = am + b$). Here $\sigma = 25$. The narrow plots on the far right are for higher x , and a zoomed vertical scale, showing that the difference (e) has the fastest asymptotic decay (x^{-2} as opposed to x^{-1}).

$k \in P$,

$$|(F\mathbf{f})_k| \leq 2q|S_\sigma(a, b)| + 2q \leq \frac{2}{\sqrt{\alpha}} + 12q,$$

so that

$$\sum_{k \in P} (F\mathbf{f})_k^2 \leq \left(\frac{2}{\sqrt{\alpha}} + 12q \right)^2 p.$$

Defining $\mathbf{v} \in \mathbb{C}^q$ as the central q entries of \mathbf{f} just as in (2.8), and noting that the compact support of $f(t)$ makes all other entries $f_j = 0$, we have $A\mathbf{v} = (F\mathbf{f})_{k \in P}$ and

$$\|A\mathbf{v}\| = \left(\sum_{k \in P} (F\mathbf{f})_k^2 \right)^{1/2} \leq \left(\frac{2}{\sqrt{\alpha}} + 12q \right) \sqrt{p} = 2\sqrt{N}(1 + 6\sqrt{\alpha}q).$$

We combine this with the simple bound $\|\mathbf{v}\| \geq f_0 = f(0) = I_0(\sigma) - 1$, and recall $\sigma_{\min}(A) \leq \|A\mathbf{v}\|/\|\mathbf{v}\|$ for any $\mathbf{v} \neq \mathbf{0}$, to complete the proof. \square

3.1. Technical lemmas on one-sided warped sinc sums. The one-sided sum $S_\sigma(a, b)$ defined by (3.6) involves the sinc of each frequency in an algebraic progression $\{am + b\}_{m \geq 0}$, but also the sinc of each frequency in a “warped” sequence $\{\sqrt{(am + b)^2 - \sigma^2}\}_{m \geq 0}$. The proof of Theorem 10 relied on our ability to bound algebraic sums over the difference between warped and unwarped sinc functions, expressed by the main Lemma 13 below. This lemma is nontrivial, because the sum of a single sinc over a general algebraic progression is at best conditionally convergent

(because its tail decays with power -1), and may not even be finite (see Remark 11). One might hope that the *difference* between the sinc functions in (3.6) eventually has more rapid decay, because the difference in their two arguments tends to zero as $m \rightarrow \infty$. This is true—illustrated by Figure 3.1(c–e)—and is the idea behind its proof, which occupies the rest of this section.

REMARK 12. *Our technique adapts several steps from the thesis of Fourmont [14, Sec. 2.5], who showed how phased sums over a sinc whose argument is a warped algebraic progression (with offset $b = na$, $n \in \mathbb{N}$) can be bounded by the phased sum over the unwarped sinc. This requires decomposing the sinc function into numerator and denominator factors, and showing how the effect of warping each factor becomes small for large enough m . His task was to bound the aliasing error in the non-uniform FFT algorithm when using (3.2) as a spreading kernel [15]. Our task is in one way simpler because there is no phase, but we also need to handle general b .*

LEMMA 13. *Let $a \geq \pi$, $\sigma \in (0, a/2)$, and $b > \sigma$. Then*

$$|S_\sigma(a, b)| = \left| \sum_{m \geq 0} \operatorname{sinc} \sqrt{(am + b)^2 - \sigma^2} - \operatorname{sinc}(am + b) \right| \leq \frac{5}{2a\sqrt{\alpha}} + 5, \quad (3.8)$$

where $\alpha = 1 - 2\sigma/a \in (0, 1)$.

Note that we use the symbol α here since it is consistent with (3.5) when $a = \pi q$, as occurs when this lemma is applied above in (3.7).

Proof. From now on we use $x = am + b$ to denote a frequency in the progression. Then, since $x > 0$,

$$\begin{aligned} S_\sigma(a, b) &= \sum_{m \geq 0} \frac{\sin \sqrt{x^2 - \sigma^2}}{\sqrt{x^2 - \sigma^2}} - \frac{\sin x}{x} \\ &= \sum_{m \geq 0} \sin \sqrt{x^2 - \sigma^2} \left(\frac{1}{\sqrt{x^2 - \sigma^2}} - \frac{1}{x} \right) + \frac{\sin \sqrt{x^2 - \sigma^2} - \sin x}{x}, \end{aligned} \quad (3.9)$$

which is Fourmont’s decomposition. By the triangle inequality, and using that $|\sin y| \leq 1$,

$$|S_\sigma(a, b)| \leq \sum_{m \geq 0} \left| \frac{1}{\sqrt{x^2 - \sigma^2}} - \frac{1}{x} \right| + \sum_{m \geq 0} \left| \frac{\sin \sqrt{x^2 - \sigma^2} - \sin x}{x} \right|.$$

We apply the “denominator warp” Proposition 14 stated below (using $y = a/2$ and the definition of α) to the first summand. We also apply the “numerator warp” Lemma 15 stated below, which applies since $a \geq \pi$, to bound the second sum by 5. We then split off the first term of the remaining sum and bound the rest by an integral:

$$\begin{aligned} |S_\sigma(a, b)| &\leq \frac{\sigma^2}{\sqrt{\alpha}} \sum_{m \geq 0} \frac{1}{x^3} + 5 \leq \frac{\sigma^2}{\sqrt{\alpha}b^3} + \frac{\sigma^2}{\sqrt{\alpha}} \sum_{m > 0} \frac{1}{x^3} + 5 \\ &\leq \frac{2}{a\sqrt{\alpha}} + \frac{\sigma^2}{\sqrt{\alpha}} \cdot \frac{1}{a} \int_b^\infty \frac{dx}{x^3} + 5 \leq \frac{2}{a\sqrt{\alpha}} + \frac{1}{2a\sqrt{\alpha}} + 5, \end{aligned} \quad (3.10)$$

where in the final two steps we used $1/b < 2/a$ and $\sigma/b < 1$. \square

The rest of this subsection is devoted to the required bounds on the effect of warping on the numerator and denominator of the sinc function. The first estimate

shows that the effect of warping the denominator is $\mathcal{O}(x^{-3})$ as frequency $x \rightarrow \infty$, with an explicit constant.

PROPOSITION 14 (Denominator warp). *Fix $\sigma > 0$ and $y > \sigma$, then*

$$\frac{1}{\sqrt{x^2 - \sigma^2}} - \frac{1}{x} \leq \frac{\sigma^2}{\sqrt{1 - \sigma/y}} \cdot \frac{1}{x^3}, \quad \text{for all } x \geq y. \quad (3.11)$$

Proof. Since $x > \sigma$, expanding the left side gives

$$\frac{1 - \sqrt{1 - (\sigma/x)^2}}{x\sqrt{1 - (\sigma/x)^2}} = \frac{(\sigma/x)^2}{x\sqrt{1 - (\sigma/x)^2}(1 + \sqrt{1 - (\sigma/x)^2})} \leq \frac{\sigma^2}{\sqrt{1 - \sigma/x}} \cdot \frac{1}{x^3},$$

and applying $x \geq y$ to the first factor gives the result. \square

The following shows that the effect of warping the numerator on the sum is uniformly bounded over the allowed set of parameters σ, a, b . Its proof needs several results which complete the subsection.

LEMMA 15 (Numerator warp). *Let $a \geq \pi$, $\sigma \in (0, a/2)$, and $b \geq a/2$. Then, using the abbreviation $x = am + b$,*

$$\sum_{m \geq 0} \left| \frac{\sin \sqrt{x^2 - \sigma^2} - \sin x}{x} \right| \leq 5. \quad (3.12)$$

Proof. Fixing σ , will make frequent use of the frequency warping deviation function,

$$R(x) := x - \sqrt{x^2 - \sigma^2}, \quad x \geq \sigma. \quad (3.13)$$

Now, noting $\sin \sqrt{x^2 - \sigma^2} = \sin(x - R(x))$, applying the addition formula, subtracting $\sin x$ from both sides and dividing by x gives

$$\frac{\sin \sqrt{x^2 - \sigma^2} - \sin x}{x} = \sin x \frac{\cos R(x) - 1}{x} - \cos x \frac{\sin R(x)}{x}.$$

Applying the triangle inequality termwise, and bounds on \sin and \cos , gives

$$\sum_{m \geq 0} \left| \frac{\sin \sqrt{x^2 - \sigma^2} - \sin x}{x} \right| \leq \sum_{m \geq 0} \left| \frac{\cos R(x) - 1}{x} \right| + \sum_{m \geq 0} \left| \frac{\sin R(x)}{x} \right| \leq 3 + 2,$$

by Lemmas 17 and 16 respectively. \square

LEMMA 16. *Let $a \geq \pi$, $\sigma \in (0, a/2)$, and $b \geq a/2$. Then, with $R(x)$ as in (3.13), and using the abbreviation $x = am + b$,*

$$\sum_{m \geq 0} \left| \frac{\sin R(x)}{x} \right| \leq 2. \quad (3.14)$$

Proof. By Proposition 18 below, $R(x) = \mathcal{O}(x^{-1})$ so that the tail of the sum is $\mathcal{O}(x^{-2})$ and hence summable. However, this only becomes useful for sufficiently large m . Thus the idea will be to split the sum at index $m_0 := \lceil \sigma^2/a \rceil \geq 1$, chosen so that, given the hypotheses on σ, a , and b ,

$$R(x) \leq \frac{\sigma^2}{x} \leq 1, \quad \text{for all } m \geq m_0. \quad (3.15)$$

This follows easily from the fact that $x = am + b \geq am_0 + b \geq \sigma^2 + b$, that $b > \sigma$, and from Proposition 18. For the first m_0 terms we use the crude bound $|\sin R(x)| \leq 1$, but use $\sin y \leq y$ for $0 < y \leq 1$ and (3.15) in the tail sum, and get

$$\sum_{m \geq 0} \left| \frac{\sin R(x)}{x} \right| \leq \sum_{m=0}^{m_0-1} \left| \frac{\sin R(x)}{x} \right| + \sum_{m \geq m_0} \left| \frac{\sin R(x)}{x} \right| \leq \sum_{m=0}^{m_0-1} \frac{1}{x} + \sigma^2 \sum_{m \geq m_0} \frac{1}{x^2}. \quad (3.16)$$

After splitting off its first term, we bound the rest of the finite sum by an integral with upper limit $a(m_0 - 1) + b < \sigma^2 + b$

$$\begin{aligned} \sum_{m=0}^{m_0-1} \frac{1}{am+b} &\leq \frac{1}{b} + \frac{1}{a} \int_b^{b+\sigma^2} \frac{dx}{x} \leq \frac{2}{a} + \frac{1}{a} \log(1 + \sigma^2/b) \leq \frac{2}{a} + \frac{1}{a} \log(1 + a/2) \\ &\leq \frac{2}{\pi} + \frac{1}{\pi} \log(1 + \pi/2) \leq 1, \end{aligned} \quad (3.17)$$

where the replacement of a by its lower limit π is justified by checking that the function of a has negative derivative for all $a > 0$. The infinite sum in (3.16) is similarly bounded by an integral

$$\sigma^2 \sum_{m \geq m_0} \frac{1}{(am+b)^2} \leq \frac{\sigma^2}{(am_0+b)^2} + \frac{\sigma^2}{a} \int_{b+\sigma^2}^{\infty} \frac{dx}{x^2} \leq \frac{\sigma^2}{a^2} + \frac{1}{a} \leq 1,$$

using $\sigma \leq a/2$ and $a \geq \pi$. Adding the two above bounds completes the proof. \square

LEMMA 17. *Let $a \geq \pi$, $\sigma \in (0, a/2)$, and $b \geq a/2$. Then, with $R(x)$ as in (3.13), and using the abbreviation $x = am + b$,*

$$\sum_{m \geq 0} \left| \frac{\cos R(x) - 1}{x} \right| \leq 3. \quad (3.18)$$

Proof. The proof is very similar to that of Lemma 16. We choose m_0 in the same way. Then for all $m \geq m_0$, since $R(x) \leq 1$ then, by Taylor's theorem followed by Proposition 18,

$$|\cos R(x) - 1| \leq \frac{R(x)^2}{2} \leq \frac{\sigma^4}{2x^2}.$$

Again splitting the sum, and bounding the first m_0 terms via $|\cos R(x) - 1| \leq 2$, and the rest via the above formula,

$$\sum_{m \geq 0} \left| \frac{\cos R(x) - 1}{x} \right| \leq \sum_{m=0}^{m_0-1} \frac{2}{x} + \frac{\sigma^4}{2} \sum_{m \geq m_0} \frac{1}{x^3}.$$

The first sum is no more than 2, using (3.17). The second sum we bound by its first term plus an integral to get

$$\frac{\sigma^4}{2} \sum_{m \geq m_0} \frac{1}{(am+b)^3} \leq \frac{\sigma^4}{2(am_0+b)^3} + \frac{\sigma^4}{2a} \int_{b+\sigma^2}^{\infty} \frac{dx}{x^3} \leq \frac{\sigma^4}{(am_0+b)^2} \cdot \frac{1}{2a} + \frac{\sigma^4}{2a} \cdot \frac{1}{2\sigma^4} \leq 1,$$

using $\sigma^2 < am_0 + b$, $\sigma \leq a/2$ and $a \geq \pi$. Adding these two bounds finishes the proof. \square

Finally, the above two proofs relied on the following fact that the effect of warping the numerator is $\mathcal{O}(x^{-1})$.

PROPOSITION 18. *Let $\sigma \geq 0$ and $R(x) := x - \sqrt{x^2 - \sigma^2}$ as in (3.13). Then $R(x) \leq \sigma^2/x$ for all $x \geq \sigma$.*

Proof. Since $\sigma < x$, we expand

$$R(x) = x(1 - \sqrt{1 - (\sigma/x)^2}) = \frac{x \cdot (\sigma/x)^2}{1 + \sqrt{1 - (\sigma/x)^2}} \leq \frac{\sigma^2}{x}.$$

□

4. Proof of improved rate for small α and β (Theorem 3). As with the other two main theorems, Theorem 3 combines a lower bound on $\sigma_1(A)$ (Proposition 5) and an upper bound on $\sigma_{\min}(A)$, in this case the following lemma.

LEMMA 19. *Let A be a cyclically contiguous $p \times q$ submatrix of the $N \times N$ discrete Fourier matrix F , with $1 < q \leq p < 4N/\epsilon\pi + 1$. Then*

$$\sigma_{\min}(A) \leq \frac{2\sqrt{pq}}{1 - (\epsilon\pi(p-1)/4N)} \left(\frac{\epsilon\pi(p-1)}{4N} \right)^{q-1}. \quad (4.1)$$

Proof. Following [31, Lem. 3.2] we start with the Bessel–Chebyshev expansion

$$e^{ixt} = J_0(x) + \sum_{n=1}^{\infty} 2i^n J_n(x) T_n(t), \quad \text{uniformly for } x \in \mathbb{R}, |t| \leq 1, \quad (4.2)$$

arising by inserting $t = \cos \theta$ into the Jacobi–Anger expansion $e^{ix \cos \theta} = \sum_{n \in \mathbb{Z}} i^n J_n(x) e^{in\theta}$. The submatrix elements can be generated by sampling this kernel on the product of the regular grids $x_j = (-1 + 2j/(p-1))W$, $j = 1, \dots, p$ and $t_k := -1 + 2k/(q-1)$, $k = 1, \dots, q$. Scaling the x -domain size by setting $W = \pi(q-1)(p-1)/2N$ insures that the matrix with elements $A_{jk} = e^{ix_j t_k}$ is, up to irrelevant left and right multiplication by diagonal unitary matrices, equal to any given $p \times q$ contiguous submatrix of the size- N Fourier matrix F . Defining for $n = 0, 1, \dots$ the sequences of vectors $\mathbf{u}_n \in \mathbb{C}^p$ and $\mathbf{v}_n \in \mathbb{C}^q$, with elements $(\mathbf{u}_0)_j \equiv 1$, $(\mathbf{u}_n)_j := 2i^n J_n(x_j)$ for $n = 1, 2, \dots$, and $(\mathbf{v}_n)_k := T_n(t_k)$ for $n = 0, 1, \dots$, we rewrite the matrix of samples of (4.2) as the sum of rank-1 outer products

$$A = \sum_{n=0}^{\infty} \mathbf{u}_n \mathbf{v}_n^*.$$

Since $q \leq p$, then $\sigma_{\min}(A) = \sigma_q(A)$. The rank approximation theorem (e.g., [17, Thm. 2.5.3]) bounds

$$\begin{aligned} \sigma_{\min}(A) &\leq \left\| A - \sum_{n=0}^{q-2} \mathbf{u}_n \mathbf{v}_n^* \right\| = \left\| \sum_{n=q-1}^{\infty} \mathbf{u}_n \mathbf{v}_n^* \right\| \leq \sum_{n=q-1}^{\infty} \|\mathbf{u}_n\| \|\mathbf{v}_n\| \\ &\leq 2\sqrt{pq} \sum_{n=q-1}^{\infty} \max_{0 \leq x \leq W} |J_n(x)| \leq 2\sqrt{pq} \sum_{n=q-1}^{\infty} [g(W/n)]^n, \quad \text{if } q-1 > W, \end{aligned}$$

where in the penultimate step we used $|T_n(t)| \leq 1$, and in the last step Siegel's bound for $J_n(nz)$ [30, 10.14.5] where $g(z) := ze^{\sqrt{1-z^2}}/(1 + \sqrt{1-z^2})$, for $z = x/n \leq 1$. Note

that $q - 1 > W$ is equivalent to $p < 2N/\pi + 1$ which holds by the hypotheses of the lemma. We now observe that $g(z) \leq ez/2$ in $0 < z \leq 1$, bound $g(W/n)$ by $g(W/(q - 1))$, and recall $W/(q - 1) = \pi(p - 1)/2N < 1$, to get

$$\sigma_{\min}(A) \leq 2\sqrt{pq} \sum_{n=q-1}^{\infty} \left(\frac{e\pi(p-1)}{4N} \right)^n,$$

a bounded geometric sum when $(p - 1)/N < 4/e\pi$, a hypothesis of the lemma, giving (4.1). \square

REMARK 20. *We initially tried the low-rank expansion of e^{ixt} resulting from the Taylor series for e^z , following [10, Lem. 1], but found that this gave a rate replacing the exponential term in (4.1) with $[e\pi(p - 1)/2N]^{q-1}$, which is exactly half the rate in (4.1), and even weaker than (1.5). It is therefore possible that yet other low-rank expansions, such as the double-Chebyshev [34, App. A], could further improve the rate in the corner region $\alpha, \beta \ll 1$.*

5. Discussion.

5.1. Numerical study of sharpness of exponential rate bounds. Figure 1.1 showed $\text{cond}(A)$ for various fixed submatrices A , at small N . However, Theorems 1–3 may be seen as lower bounds on the *asymptotic* exponential growth rate with respect to N , for fixed shape (α, β) , as summarized in Table 1.1. Thus we numerically measured the *empirical* asymptotic growth rate $\tilde{\rho}(\alpha, \beta)$ along the family of submatrices sharing a given (α, β) , but growing N , to see how close our lower bounds were to this rate. The result is Figure 4.1. Comparing its panels (a) and (b) shows that (the symmetrized) Theorem 2 captures well the main features of the empirical rate. Indeed, the ratio $\tilde{\rho}/\rho$, plotted in (c), is less than 1.2 in 54% of the area of the square $(0, 1)^2$. This ratio approaches 1 in the neighborhoods of $(1, 0)$ and $(0, 1)$, as expected since Theorem 2 has a sharp rate there (Remark 4). However, in quite a tight band around the diagonal $\alpha = \beta$ the empirical rate exceeds this lower bound by a significant factor. This factor is about 1.45 at $(1/2, 1/2)$, and along the diagonal grows slowly but without bound as the corners $(0, 0)$ and $(1, 1)$ are approached.

However, we know that the rate of Theorem 3 beats that of Theorem 2 inside the corner $(0, \alpha_*)^2$, where $\alpha_* \approx 0.117$ (see Section 1.1). Hence, in Figure 4.1(d–f) we zoom in to the neighborhood of this region, comparing the empirical rate to the stronger of these two theorems (their cross-over at $\max(\alpha, \beta) = \alpha_*$ is visible as kinks in the contour lines in (e) and (f)). As panel (f) shows, the ratio now appears *uniformly* bounded, reaching its maximum at $\alpha = \beta = \alpha_*$. An estimate of this maximum is given by the ratio at $(0.12, 0.12)$, which is less than 1.91. As $\beta \rightarrow 0$, the ratio peaks at a value about 1.7 at $\alpha = \alpha_*$. As $(\alpha, \beta) \rightarrow (0, 0)$, the ratio drops. Remark 4 on the prolate asymptotic suggests that the ratio tends to 1 (logarithmically slowly) if approached along the axes.

REMARK 21 (measuring the empirical rate $\tilde{\rho}(\alpha, \beta)$). *Generating Figure 4.1 needed an accurate measurement of the constant $\tilde{\rho}$ in the asymptotic model $\text{cond}(A) \sim ce^{\tilde{\rho}N}$ as $N \rightarrow \infty$. Recall that here A takes a sequence of integer sizes $p \times q$ with $p/N = \alpha$ and $q/N = \beta$ fixed (and, thus, rational). This places constraints on the allowable p and q , making the measurement subtle. As an example, to estimate $\tilde{\rho}(0.5, 0.49)$ the smallest possible case of A is a 50×49 submatrix with $N = 100$, and yet already $\text{cond}(A) > 10^{16}$, exceeding the value reliably measurable in double-precision arithmetic.*

There are two ways out of this quandary: either compute SVDs via a higher precision arithmetic library, or limit oneself to α and β with small rational denominators.

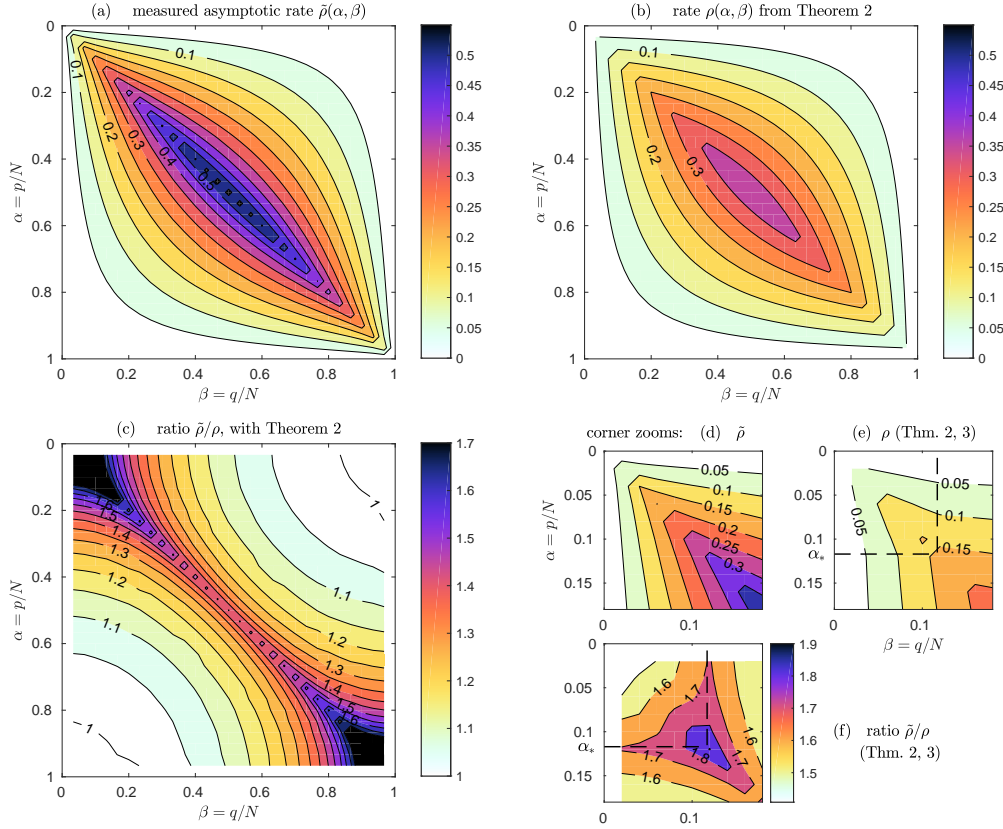


FIG. 4.1. Comparison of exponential growth rates with N of the condition number of a $p \times q$ submatrix of the size- N Fourier matrix, as a function of shape parameters $\alpha := p/N$ and $\beta := q/N$. The α axis increases downward to match the usual matrix convention. (a) shows contours of the numerically-measured rate, fitting the model $\text{cond}(A) \approx Ce^{\tilde{\rho}(\alpha, \beta)N}$, for (α, β) sampled on a grid of spacing $1/30$; see Remark 21. (b) shows the lower bound $\rho = \frac{\pi}{2}[\min(\alpha, \beta) - \alpha\beta]$ from Theorem 2. (c) shows the ratio of (a) to (b), i.e., the sharpness of the theorem. The breakup into small dots along the diagonals of (a) and (c) are contouring artifacts. Panels (d,e,f) show a zoom around the origin of panels (a,b,c) respectively, on a grid of spacing $1/50$, but also applying Theorem 3 in the corner $(0, \alpha_*)^2$ (shown dotted), where it is stronger than Theorem 2.

We opted for the latter. This led to the choices of $1/30$ and $1/50$ for the grid spacings in Figure 4.1, which were adequate. We wrote a simple code which, given such a pair (α, β) , uses a bisection search along the family of A with this shape, identifying the largest A for which $\text{cond}(A)$ does not exceed an upper limit of around 10^{16} . This data point is combined with another taken from the A nearest to half this size (giving $\text{cond}(A) \sim 10^8$, bypassing any pre-asymptotic growth). The $\tilde{\rho}$ returned is the slope between (the log of) these two points. The accuracy is around ± 0.02 , estimated by comparing equivalent rational forms for (α, β) . The code ran in MATLAB R2017a on a laptop with Intel i7 CPU, taking a few seconds to generate all figures in this paper. Certainly a more elaborate arbitrary-precision code could be built, but the above served our purposes well.

The code described above, plus those generating the other figures in this paper, can be found at <https://github.com/ahbarnett/fourier-submat>

5.2. Symmetry and near-symmetry in the (α, β) plane. The empirical rate plot Figure 4.1(a) appears to have two symmetries (i.e. the D_2 dihedral group).

The first is that $\text{cond}(A)$ is invariant to the diagonal reflection $(\alpha, \beta) \mapsto (\beta, \alpha)$, which follows immediately from the fact that a submatrix of swapped dimensions is the adjoint, and $\text{cond}(A)^* = \text{cond}(A)$.

The second symmetry in Figure 4.1(a) is that the rate also appears invariant under $(\alpha, \beta) \mapsto (1 - \alpha, 1 - \beta)$, i.e., inversion about $(1/2, 1/2)$, or complementing both row and column index sets. However, understanding this is more subtle. From the rate one might suspect that $\text{cond}(A)$ itself is also invariant under changing the submatrix from size $p \times q$ to $(N - p) \times (N - q)$. But this cannot be true, as the case $p = q = 1$ shows: the condition number of any 1×1 matrix is unity, and letting A now be a $(N - 1) \times (N - 1)$ submatrix of F gives $\sigma_1(A) = \sqrt{N}$ by the interlacing property (e.g. [39, Thm. 1]). Choosing the omitted row and column to be $j = k = 0$, it is easy to check that A acting on the vector of all ones is sent to the negative of this vector, showing $\sigma_{\min}(A) \leq 1$ and $\text{cond}(A) \geq \sqrt{N}$ (this turns out to be an equality), which is certainly not unity!

The condition number of a submatrix of F is *not* invariant with respect to complementing its dimensions $p \times q$ to give $(N - p) \times (N - q)$, yet as N grows this becomes a *near* symmetry. Figure 1.1 shows how strikingly rapid this is: even at $N = 8$ the near-symmetry is clear, and by $N = 16$ the *failure* of symmetry is almost impossible to see. This seems quite mysterious until we spot the following identity.

PROPOSITION 22. *Let A be a $p \times q$ submatrix of F with $p + q < N$, and let D be the $(N - p) \times (N - q)$ submatrix of F defined by the complement of the row and column index sets of A . Then*

$$\frac{\text{cond}(A)}{\text{cond}(D)} = \sqrt{1 - \frac{(\sigma_{\min}(C))^2}{N}}, \quad (5.1)$$

where C is the $(N - p) \times q$ submatrix of F with the same column indices as A , and the complement of the row indices.

Proof. If $p < q$ then we apply the diagonal reflection symmetry, so that we can from now take $p \geq q$. We apply a permutation moving A to the upper left position in F , which does not change $\text{cond}(A)$ nor $\text{cond}(D)$, then label the blocks as above, with the missing fourth block named B :

$$F \begin{bmatrix} \mathbf{v} \\ \mathbf{0} \end{bmatrix} = \begin{bmatrix} A & B \\ C & D \end{bmatrix} \begin{bmatrix} \mathbf{v} \\ \mathbf{0} \end{bmatrix} = \begin{bmatrix} \mathbf{u} \\ \mathbf{w} \end{bmatrix}.$$

The rest is simple singular value inequalities. If \mathbf{v} is the normalized minimum right singular vector for A , then because A is square or “tall”, $\|\mathbf{u}\| = \|A\mathbf{v}\| = \sigma_{\min}$ is as small as possible over unit vectors $\mathbf{v} \in \mathbb{C}^q$. However, by isometry of F , $\|\mathbf{u}\|^2 + \|\mathbf{w}\|^2 = N$, so that $\|\mathbf{w}\| = \|C\mathbf{u}\|$ is the largest possible, hence \mathbf{v} is also the normalized maximum right singular vector for C . Thus

$$(\sigma_{\min}(A))^2 + (\sigma_{\max}(C))^2 = N. \quad (5.2)$$

Swapping the words “minimum” and “maximum” in this argument requires additionally that C not be “fat”, which is true by the assumption $q < N - p$. This gives

$$(\sigma_{\max}(A))^2 + (\sigma_{\min}(C))^2 = N. \quad (5.3)$$

We now reason similarly for the blocks of $F^* = [A^*, C^*; B^*, D^*]$, multiplying it against $[\mathbf{0}; \mathbf{v}]$ to sample its right two blocks. By the assumption, D^* is not fat, so may play the role of A in (5.2), giving

$$(\sigma_{\min}(D))^2 + (\sigma_{\max}(C))^2 = N . \quad (5.4)$$

However, C^* is fat, so the minimum of $\|C^* \mathbf{v}\|$ over unit-norm $\mathbf{v} \in \mathbb{C}^q$ is zero, leaving

$$(\sigma_{\max}(D))^2 = N . \quad (5.5)$$

Combining (5.2) and (5.4) shows $\sigma_{\min}(A) = \sigma_{\min}(D)$. Thus the left-hand side of (5.1) is $\sigma_{\max}(A)/\sigma_{\min}(D)$, and inserting (5.5) and (5.3) completes the proof. \square

This proposition means that $\text{cond}(A)$ for a submatrix shape (α, β) in the triangle $\alpha + \beta < 1$ is *strictly* smaller than $\text{cond}(A)$ for its inverted shape $(1 - \alpha, 1 - \beta)$. However, the relative difference between the two condition numbers vanishes as C , itself a submatrix of shape $(1 - \alpha, \beta)$, becomes highly ill-conditioned. Since as N grows this happens everywhere except $\alpha, \beta \approx 0$, the mystery of the near-symmetry of Figure 1.1 is explained. By the lower bound of Theorem 1 or 2 this occurs eventually for any $(\alpha, \beta) \in (0, 1)^2$, proving that the true *asymptotic* exponential growth rate is exactly inversion symmetric.

Intriguingly, the rates in Theorems 1 and 2 also obey this inversion symmetry; in their proofs this can be traced to the fixed ‘‘Heisenberg’’ product of the sizes of the sets \overline{P} and Q (e.g. see Figure 1.2(b), and (3.5)). Yet Theorem 3 cannot obey it, because its maximum α allowed is less than $1/2$. However, combining it with Proposition 22 allows it to be also applied near the $(1, 1)$ corner, as follows.

COROLLARY 23. *The lower bound on exponential rates given in the last row of Table 1.1 also apply with the replacement of (α, β) by $(1 - \alpha, 1 - \beta)$, in the region $\alpha, \beta > 1 - 4/e\pi$.*

5.3. Conclusions and open problems. Fourier submatrices are quite elementary objects, arising in many applications, yet until now there have been very few rigorous bounds on their conditioning. Our new non-asymptotic lower bounds on the condition number of a $p \times q$ submatrix of the size- N Fourier matrix apply to all N and, when combined with the obvious $p \leftrightarrow q$ symmetry, essentially all p and q . All constants are explicit. Interpreted as asymptotic results for p and q fixed fractions of N , as $N \rightarrow \infty$, they give exponential lower bounds with rates listed in Table 1.1. Numerical study (Section 5.1) shows that their rates capture quite well the empirical growth, which is also exponential, uniformly over shape space. Section 5.2 explained a non-obvious symmetry effect in this space.

As an example application of our results, in 1D Fourier extension with the parameters $T = \gamma = 2$ recommended by [1], the exponential growth rate⁷ has the bound $\rho(1/2, 1/4) \geq 3\pi/16$, by applying Theorem 2.

Our methods are elementary: Theorem 1 used a Gaussian trial vector, Theorem 2 a more sophisticated trial vector and quite detailed estimates, while Theorem 3, applying only in the ‘‘corner’’ region of small α and β , used the SVD rank approximation theorem. In Theorem 2, we achieved a rate that is *sharp* in the limit $(\alpha, \beta) \rightarrow (1, 0)$, or $(0, 1)$, due to using the (deplinthed) Kaiser–Bessel pair (3.3). This shares with the prolate spheroidal wavefunctions an optimal frequency localization rate in $L^2(\mathbb{R})$, but is more accessible. We suspect that this is its first use as a pure analysis tool.

⁷In the notation of [1], $\kappa(\overline{A})$ grows at least as fast as $e^{3\pi N/2}$, up to algebraic prefactors.

Our rate is *not* sharp long the axis $(\alpha, 0)$, or $(0, \beta)$, but possibly could be made so by using a discrete prolate spheroidal sequence (DPSS) [35] as the trial vector \mathbf{v} . This would require estimating *finite sums* over the tails of $H(\omega)$ in [35], for which only asymptotics are known. It is also unclear whether this would simply duplicate (1.6). Another approach would be to extend the methods of [41]. Also see Remark 20.

This paper studied lower bounds in depth; we did not address upper bounds at all, which seems to be quite an open area. On this topic, for now we direct the reader to [6], and rather special cases in recent super-resolution literature: [26, Thm. 2, case $A = 1$], [5, Thm. 3.2], and [24, §4]. These references also deal with the generalization to non-uniform Fourier matrices (also see [34]). In 2D and 3D applications, Kronecker products of Fourier submatrices arise; we explore one such direction in [3].

Our numerical study suggests fascinating open problems. There appears to be a *universal* exponential rate as a function of shape, as shown in Figure 4.1(a); what is it? (Answering this would be equivalent to writing an asymptotic form for the smallest P-DPSS eigenvalue [19, 41].) In particular, what phenomenon explains the sudden spike in growth rate around the diagonal, where the submatrix tends to become square?

6. Acknowledgments. The author benefited from helpful discussions with Hannah Lawrence, Daan Huybrechs, Charlie Epstein, David Barmherzig, and Alex Townsend, and from corrections by Dominik Nagel. The Flatiron Institute is a division of the Simons Foundation.

Appendix A. Proof of the Kaiser–Bessel Fourier transform pair. Here we prove (3.2), in two steps. The first will be to establish a related Fourier transform,

$$\int_{-1}^1 J_0(b\sqrt{1-z^2})e^{ikz} dz = 2 \operatorname{sinc} \sqrt{k^2 + b^2}, \quad \text{for } b \in \mathbb{R}, k \in \mathbb{R}. \quad (\text{A.1})$$

This is equivalent to a formula in Gradshteyn–Ryzhik [18, 6.677(6)], although neither of the books cited therein prove it or give a reference; the scent goes cold. We prove it simply by *averaging a plane wave over the unit sphere*. The second step will analytically continue this formula to imaginary b .

Proof. We insert the integral representation [30, (10.9.1)] of the Bessel function $J_0(s) = (2\pi)^{-1} \int_0^{2\pi} e^{is \sin \phi} d\phi$ into the left-hand side of (A.1), then change variable $z = \cos \theta$, thus

$$\begin{aligned} \int_{-1}^1 J_0(b\sqrt{1-z^2})e^{ikz} dz &= \frac{1}{2\pi} \int_{-1}^1 \int_0^{2\pi} e^{ib\sqrt{1-z^2} \sin \phi} e^{ikz} d\phi dz \\ &= \frac{1}{2\pi} \int_0^\pi \int_0^{2\pi} e^{ib \sin \theta \sin \phi + ik \cos \theta} \sin \theta d\phi d\theta = \frac{1}{2\pi} \int_{S^2} e^{i(0,b,k) \cdot (x,y,z)} dS_{(x,y,z)} \\ &= \frac{1}{2\pi} \int_{S^2} e^{i\sqrt{k^2+b^2}z} dS_{(x,y,z)} = \int_{-1}^1 e^{i\sqrt{k^2+b^2}z} dz = 2 \operatorname{sinc} \sqrt{k^2 + b^2}, \end{aligned}$$

proving (A.1). The key step passing to the last line is invariance of the mean under rotation of the coordinate system, whose new z axis points in the direction $(0, b, z)$.

Although (A.1) assumed real b , our second step shows that, fixing k , both sides are in fact entire with respect to b . This holds for the right-hand side because the square-root has singularities only at $b = \pm ik$, but these are removed by the entire function sinc having only even powers at its origin. The left-hand side is entire because the integrand is entire for each z and continuous in (b, z) , so one may apply [37, Thm. 5.4,

Ch. 2]. By unique continuation the equality thus holds for all $b \in \mathbb{C}$, in particular $b = i\sigma$, so, using $I_0(s) = J_0(is)$ from [30, (10.27.6)], this gives

$$\int_{-1}^1 I_0(\sigma\sqrt{1-z^2})e^{ikz} dz = 2 \operatorname{sinc} \sqrt{k^2 - \sigma^2}.$$

Rewriting $k = 2\pi\omega$ and $z = t$ gives (3.2). \square

REFERENCES

- [1] B. Adcock, D. Huybrechs, and J. Martín-Vaquero. On the numerical stability of Fourier extensions. *Found. Comput. Math.*, 14:635–687, 2014.
- [2] N. Albin and O. P. Bruno. A spectral FC solver for the compressible Navier-Stokes equations in general domains I: Explicit time-stepping. *J. Comput. Phys.*, 230:6248–6270, 2011.
- [3] D. Barmherzig, A. H. Barnett, C. L. Epstein, L. F. Greengard, J. F. Magland, and M. Rachh. Recovering missing data in coherent diffraction imaging, 2020. preprint, [arxiv:2002.02874](https://arxiv.org/abs/2002.02874).
- [4] A. H. Barnett. Aliasing error of the $\exp(\beta\sqrt{1-z^2})$ kernel in the nonuniform fast Fourier transform, 2020. preprint [arxiv:2001.09405](https://arxiv.org/abs/2001.09405). submitted, *Appl. Comput. Harmon. Anal.*
- [5] D. Batenkov, L. Demanet, G. Goldman, and Y. Yomdin. Conditioning of partial nonuniform Fourier matrices with clustered nodes. *SIAM J. Matrix Anal. Appl.*, 41(1):199–220, 2020.
- [6] F. S. V. Bazán. Conditioning of rectangular Vandermonde matrices with nodes in the unit disk. *SIAM J. Matrix Anal. Appl.*, 21(2):679–693, 2000.
- [7] T. Bendory, R. Beinert, and Y. C. Eldar. Fourier phase retrieval: Uniqueness and algorithms. In H. Boche, G. Caire, R. Calderbank, M. März, G. Kutyniok, and R. Mathar, editors, *Compressed Sensing and its Applications (Proceedings of the Second International MATHEON Conference 2015)*, pages 55–91. Birkhäuser Basel, 2018. [arxiv:1705.09590](https://arxiv.org/abs/1705.09590).
- [8] J. P. Boyd. A comparison of numerical algorithms for Fourier extension of the first, second, and third kinds. *J. Comput. Phys.*, 178(1):118160, May 2002.
- [9] P. D. Brubeck, Y. Nakatsukasa, and L. N. Trefethen. Vandermonde with Arnoldi, 2019. submitted, *SIAM Rev.*
- [10] E. Candès, L. Demanet, and L. Ying. Fast computation of Fourier integral operators. *SIAM J. Sci. Comput.*, 29(6):2464–2493, 2007.
- [11] E. Candès and C. Fernandez-Granda. Towards a mathematical theory of super-resolution. *Commun. Pure Appl. Math.*, 67, 06 2014.
- [12] D. L. Donoho. Superresolution via sparsity constraints. *SIAM J. Math. Anal.*, 23(5):1309–1331, 1992.
- [13] A. Edelman, P. McCorquodale, and S. Toledo. The future fast Fourier transform? *SIAM J. Sci. Comput.*, 20(3):1094–1114, 1999.
- [14] K. Fourmont. *Schnelle Fourier-Transformation bei nichtäquidistanten Gittern und tomographische Anwendungen*. PhD thesis, Univ. Münster, 1999.
- [15] K. Fourmont. Non-equispaced fast Fourier transforms with applications to tomography. *J. Fourier Anal. Appl.*, 9(5):431–450, 2003.
- [16] A. Goldstein and J. Abbate. Oral history: James Kaiser. http://ethw.org/Oral-History:James_Kaiser, 1997. online; accessed 2017-04-15.
- [17] G. H. Golub and C. F. van Loan. *Matrix computations*. Johns Hopkins Studies in the Mathematical Sciences. Johns Hopkins University Press, Baltimore, MD, third edition, 1996.
- [18] I. Gradshteyn and I. Ryzhik. *Table of Integrals, Series and Products*. New York: Academic, 8th edition, 2015.
- [19] F. A. Grünbaum. Eigenvectors of a Toeplitz matrix: Discrete version of the prolate spheroidal wave functions. *SIAM J. Algeb. Discrete Methods*, 2(2):136–141, 1981.
- [20] D. Huybrechs. On the Fourier extension of nonperiodic functions. *SIAM J. Numer. Anal.*, 47(6):4326–4355, 2010.
- [21] A. Jain and S. Ranganath. Extrapolation algorithms for discrete signals with application in spectral estimation. *IEEE Trans. Acoust. Speech Signal Process.*, 29(4):830–845, 1981.
- [22] J. Kaiser. Digital filters. In J. Kaiser and F. Kuo, editors, *System analysis by digital computer*, chapter 7, pages 218–285. Wiley, 1966.
- [23] J. Keiner, S. Kunis, and D. Potts. Using NFFT 3 — a software library for various nonequispaced fast Fourier transforms. *ACM Trans. Math. Software*, 36(4), 2009.
- [24] S. Kunis and D. Nagel. On the smallest singular value of multivariate Vandermonde matrices with clustered nodes, 2019. [arxiv:1907.07119](https://arxiv.org/abs/1907.07119).

- [25] H. J. Landau and H. O. Pollak. Prolate spheroidal wave functions, Fourier analysis and uncertainty—III: the dimension of the space of essentially time- and band-limited signals. *Bell Syst. Tech. J.*, 41:1295–1336, 1962.
- [26] W. Li and W. Liao. Stable super-resolution limit and smallest singular value of restricted Fourier matrices, 2018. preprint, [arXiv:1709.03146v2](https://arxiv.org/abs/1709.03146v2) (second version).
- [27] R. Matthysen and D. Huybrechs. Fast algorithms for the computation of Fourier extensions of arbitrary length. *SIAM J. Sci. Comput.*, 38(2):A899–A922, 2016.
- [28] J. Miao, T. Ishikawa, I. K. Robinson, and M. M. Murnane. Beyond crystallography: Diffractive imaging using coherent x-ray light sources. *Science*, 348:530–535, 2015.
- [29] A. Moitra. Super-resolution, extremal functions and the condition number of Vandermonde matrices. In *Proceedings of the Forty-Seventh Annual ACM Symposium on Theory of Computing*, STOC '15, pages 821–830, New York, NY, USA, 2015. Association for Computing Machinery.
- [30] F. W. J. Olver, D. W. Lozier, R. F. Boisvert, and C. W. Clark, editors. *NIST Handbook of Mathematical Functions*. Cambridge University Press, 2010. <http://dlmf.nist.gov>.
- [31] M. O’Neil and V. Rokhlin. A new class of analysis-based fast transforms, 2007. Technical Report, YALEU/DCS/TR-1384, Yale University.
- [32] A. Osipov, V. Rokhlin, and H. Xiao. *Prolate Spheroidal Wave Functions of Order Zero: Mathematical Tools for Bandlimited Approximation*, volume 187 of *Applied Mathematical Sciences*. Springer, US, 2013.
- [33] V. Y. Pan. How bad are Vandermonde matrices? *SIAM J. Matrix Anal. Appl.*, 37(2):676–694, 2016.
- [34] D. Ruis-Antolín and A. Townsend. A nonuniform fast Fourier transform based on low rank approximation. *SIAM J. Sci. Comput.*, 40(1):A529–A547, 2018.
- [35] D. Slepian. Prolate spheroidal wave functions, Fourier analysis, and uncertainty—V: the discrete case. *Bell Syst. Tech. J.*, 57(5):1371–1430, 1978.
- [36] D. Slepian and H. O. Pollak. Prolate spheroidal wave functions, Fourier analysis and uncertainty, I. *Bell Syst. Tech. J.*, 40:43–64, 1961.
- [37] E. M. Stein and R. Shakarchi. *Complex analysis (Princeton Lectures in Analysis, No. 2)*. Princeton University Press, 2003.
- [38] E. M. Stein and R. Shakarchi. *Fourier analysis: an introduction (Princeton Lectures in Analysis, No. 1)*. Princeton University Press, 2003.
- [39] R. C. Thompson. Principal submatrices IX: Interlacing inequalities for singular values of submatrices. *Linear Algebra Appl.*, 5:1–12, 1972.
- [40] J. M. Varah. The prolate matrix. *Linear Algebra Appl.*, 187:269–278, 1993.
- [41] Z. Zhu, S. Karnik, M. A. Davenport, J. Romberg, and M. B. Wakin. The eigenvalue distribution of discrete periodic time-frequency limiting operators. *IEEE Sig. Proc. Lett.*, 25(1):95–99, 2018.